

Estimating tornado wind speed from wind turbine damage

Mahfuzur Rahman^a, Partha Sarkar^b, Sidharthan Murugan^c, Nayan Tiwari^d

^aIowa State University, Ames, IA, USA, rmahfuz@iastate.edu

^bIowa State University, Ames, IA, USA, ppsarkar@iastate.edu

^cIowa State University, Ames, IA, USA, sidhartk@iastate.edu

^dWalker Consultants, Tampa, FL, USA, ntiwari@walkerconsultants.com

SUMMARY

Estimation of tornado wind speeds is often done based on assessment of structural failure during post-storm damage surveys because measurement of tornado winds near the ground is rare. Thus, researchers rely on damage indicators and back-calculate the wind speeds that could have caused the damage. The May 21, 2024 Greenfield, Iowa tornado offered such a case study where several Vestas V110-2.0 MW wind turbines experienced tower collapse or blade failure. In this study, a failed wind turbine tower was modeled as a tapered steel cantilever tube with a lumped mass at its top and the wind loads were analytically calculated based on wind speeds at the wind turbine location using known velocity profiles and the tornado's travel path. The estimated wind speed causing the observed damage agrees with the observed wind speed and therefore demonstrates the potential use of wind turbine failure as a damage indicator for estimating tornado intensity.

Keywords: *tornado wind speed estimation, wind turbine tower failure, tornado-induced loading, structural damage indicator, tornado-structure interaction*

1. INTRODUCTION

Tornadoes are violently rotating columns of air that forms beneath a supercell thunderstorm and extend to the ground. Because they develop rapidly and follow highly erratic paths, direct in-situ tornado wind speed measurements are rare with only a handful available (e.g. Edwards et al., 2013; Lombardo et al., 2015; Kosiba and Wurman, 2023). Accurate estimation of tornado wind speeds is nevertheless essential for understanding tornado intensity, associated damage, and classification. To address this limitation, damage-based wind estimation approaches such as the Fujita scale (Fujita, 1971) and later Enhanced Fujita (EF) scale (McDonald and Mehta, 2006) were developed, relying on observed structural damage patterns. A wide range of damage indicators, including buildings, engineered structures, vegetation, and ground scouring, has since been used to infer wind speeds (Atkins et al., 2014; Kikitsu and Sarkar, 2015; Rhee and Lombardo, 2018). Comparisons of rare in-situ or radar-derived wind measurements with documented damage highlight both the value and limitations of damage-based methods and highlight the need for damage indicators with well-defined structural properties (Atkins et al., 2014; Wurman et al., 2013).

Utility-scale wind turbines represent a promising but underutilized class of engineered damage indicators. Turbine towers and nacelles are designed and manufactured with well-documented geometry, material properties, and load paths (Burton et al., 2011; Jonkman et al., 2009). Although tornado-induced failure of engineered structures, including lattice towers (Alipour et al., 2020), low-rise wood-frame buildings (Kumar et al., 2012), and wind turbines (Aslam and Alipour, 2025), have been investigated using forward structural analyses, the inverse problem of estimating tornado wind speeds directly from observed wind turbine damage has not yet been addressed.

The May 21, 2024 Greenfield, Iowa tornado provides a rare opportunity because multiple Vestas V110-2.0 MW turbines south-west of Greenfield suffered catastrophic tower collapse or blade failure. This paper investigates the use of utility-scale wind turbines as engineered damage indicators for tornado wind speed estimation. The tower is represented as a tapered tubular steel cantilever supporting the nacelle-rotor assembly as a lumped mass. Aerodynamic loads on the blades and tower are derived from a laboratory measured tornado velocity profiles obtained from the ISU-Tornado Simulator (TS). The analysis framework links observed tower failure to developed stress and structural capacity, providing a basis for relating turbine failure characteristics to the underlying wind field. To support the modeling approach, a scaled wind turbine is tested in the ISU-TS, and the measured loads are used to assess the validity of the analytical load formulation. The methodology establishes a foundation for incorporating wind turbine damage into tornado wind speed assessment.

2. METHODOLOGY

2.1. Event Overview and Damage Documentation

This study examines wind turbine damage caused by the May 21, 2024 Greenfield, Iowa tornado (EF4), which resulted in catastrophic failure of multiple Vestas V110-2.0 MW turbines west of Greenfield. Post-storm damage surveys document global tower collapse and failure at approximately one-third of the tower height from the base. The turbine considered in this study was located near the documented tornado track, and the collapse direction is consistent with strong transient lateral loading from the passing vortex. The turbine has a rotor diameter of 110 m and a hub height of 95 m. The structural steel (S355) tower is a tapered tubular steel structure with a base diameter of 5 m, and wall thickness varying from 30 mm at the base to 15 mm near the top. Tower geometry and structural properties are obtained from manufacturer data and are consistent with existing literature. The 78-ton nacelle and 22.5-ton rotor assembly are represented as a lumped mass at the tower top.

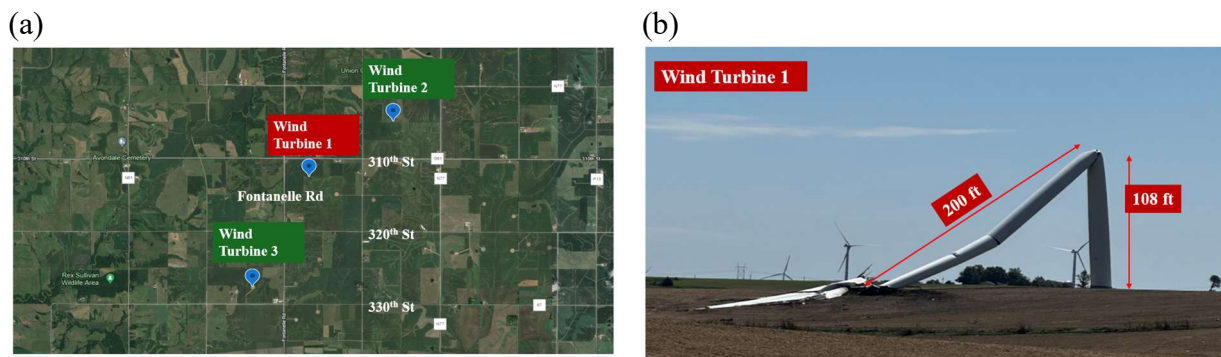


Figure 1: (a) Surveyed site on the Orient Wind Farm, (b) affected wind turbine considered in this study.

2.2. Analytical Structural Model

The wind turbine tower is modeled as a cantilever, linear elastic beam subject to time varying tornado-induced lateral loads, and a constant axial load from the self weight of the nacelle-rotor assembly, including geometric nonlinearity effects due to the axial load, and inertial load of the mass. The equation of motion of the tower at a given height (z) can be written as:

$$m(z) \frac{\partial^2 u(z,t)}{\partial t^2} + EI(z) \frac{\partial^4 u(z,t)}{\partial z^4} + P(z) \frac{\partial^2 u(z,t)}{\partial z^2} = q(z, t) \quad (1)$$

where $u(z,t)$ is lateral displacement, $m(z)$ is mass per unit height, EI is flexural rigidity, P is axial (C) load, and $q(z,t)$ is the tornado wind load. The bending moment distribution can be written as:

$$M(z, t) = EI(z) \frac{\partial^2 u(z, t)}{\partial z^2} \quad (2)$$

from which the corresponding longitudinal bending stress can be calculated as $\sigma(z, t) = \frac{M(z,t)c(z)}{I(z)}$

where $c(z)$ is the distance from the neutral axis to the extreme fiber and $I(z)$ is the second moment of area. Structural failure is assumed to initiate where the peak stress reaches material capacity.

2.3. Tornado Wind Loading and Experimental Validation

Tornado induced aerodynamic loading is derived from the measured velocity fields at ISU-TS, which produces an EF4 like vortex (swirl ratio 0.5, vane angle 55° , inflow height 0.66 m, core radius 0.41 m). Measured velocity profiles are used to calculate time varying mean and turbulent wind loads on the wind turbine components using an aerodynamic loads formulation to compute the transient structural response. An inverse analysis is performed by iteratively adjusting tornado wind speed until the analytically predicted stress demand reaches the observed failure condition. To assess the analytical loading formulation, a geometrically scaled turbine model is tested in the ISU-TS, and measured base forces are compared with analytical predictions under equivalent flow conditions.

3. PRELIMINARY RESULTS

Figure 2 shows the predicted bending stress distribution along the tower height for rotor blade orientations corresponding to maximum and minimum aerodynamic loading, reflecting the effects of varying direction of tornado winds relative to turbine alignment. For the same peak stress level, minimum turbine loading shifts the location of maximum stress downward along the tower. In both cases, peak stress occurs away from the tower base, indicating that failure initiation is governed by distributed loading and axial force induced geometric nonlinearity rather than base moment alone. These results demonstrate that blade orientation significantly alters predicted failure height and can influence damage-based tornado wind speed estimation.

4. FUTURE WORK

The preliminary results are limited to steady loading cases representing the upper and lower bounds of rotor loading conditions. Ongoing work will extend this to fully transient analysis in which the tornado translates past the turbine, which will allow the time varying internal forces and stresses to be resolved. Additional analyses will examine the influence of initial blade position, tornado approach direction, and turbine distance from the center of the tornado on the tower failure location. To support and validate the analytical framework, a geometrically scaled wind turbine model will be tested in the ISU-TS under a controlled tornado-like vortex. These efforts will allow a more complete assessment of the interaction of a wind turbine with a tornado and improved confidence in damage-based wind speed estimation.

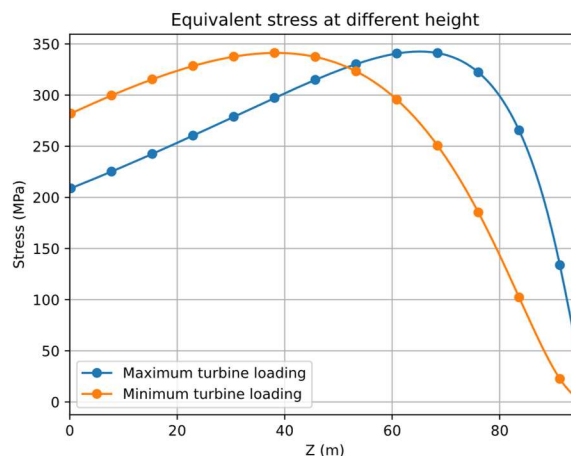


Figure 2: Equivalent bending stress distribution for maximum and minimum turbine loading cases.

ACKNOWLEDGEMENTS

This research was supported by the U.S. National Science Foundation under Award No. 2330150, “Mid-scale RI-1 (M1:DP): National Testing Facility for Enhancing Wind Resiliency of Infrastructure in Tornado-Downburst-Gust Front Events (NEWRITE).”

REFERENCES

- Alipour, A., Sarkar, P., Dikshit, S., Razavi, A., Jafari, M., 2020. Analytical Approach to Characterize Tornado-Induced Loads on Lattice Structures. *Journal of Structural Engineering* 146, 04020108. [https://doi.org/10.1061/\(ASCE\)ST.1943-541X.0002660](https://doi.org/10.1061/(ASCE)ST.1943-541X.0002660)
- Aslam, M.U., Alipour, A., 2025. Structural failure analysis of wind turbines to tornadoes in Greenfield tornadoes of 2024. *Engineering Failure Analysis* 110387. <https://doi.org/10.1016/j.engfailanal.2025.110387>
- Atkins, N.T., Butler, K.M., Flynn, K.R., Wakimoto, R.M., 2014. An Integrated Damage, Visual, and Radar Analysis of the 2013 Moore, Oklahoma, EF5 Tornado. <https://doi.org/10.1175/BAMS-D-14-00033.1>
- Burton, T., Jenkins, N., Sharpe, D., Bossanyi, E., 2011. *Wind energy handbook*. John Wiley & Sons.
- Edwards, R., LaDue, J.G., Ferree, J.T., Scharfenberg, K., Maier, C., Coulbourne, W.L., 2013. Tornado Intensity Estimation: Past, Present, and Future. <https://doi.org/10.1175/BAMS-D-11-00006.1>
- Fujita, T.T., 1971. Proposed characterization of tornadoes and hurricanes by area and intensity (No. NASA-CR-125545).
- Jonkman, J., Butterfield, S., Musial, W., Scott, G., 2009. Definition of a 5-MW Reference Wind Turbine for Offshore System Development (No. NREL/TP-500-38060). National Renewable Energy Laboratory (NREL), Golden, CO. <https://doi.org/10.2172/947422>
- Kikitsu, H., Sarkar, P.P., 2015. Building Damage, Wind Speed Estimation, and Post Disaster Recovery in an EF5 Tornado. *Natural Hazards Review* 16, 04014019. [https://doi.org/10.1061/\(ASCE\)NH.1527-6996.0000156](https://doi.org/10.1061/(ASCE)NH.1527-6996.0000156)
- Kosiba, K., Wurman, J., 2023. The strongest winds in tornadoes are very near the ground. *Commun Earth Environ* 4, 50. <https://doi.org/10.1038/s43247-023-00716-6>
- Kumar, N., Dayal, V., Sarkar, P.P., 2012. Failure of wood-framed low-rise buildings under tornado wind loads. *Engineering Structures* 39, 79–88. <https://doi.org/10.1016/j.engstruct.2012.02.011>
- Lombardo, F., Brown, T., Levitan, M., LaDue, J., 2015. Estimating Wind Speeds in Tornadoes and other Windstorms: Development of an ASCE Standard. NIST.
- McDonald, J.R., Mehta, K.C., 2006. A recommendation for an Enhanced Fujita scale (EF-Scale). Wind Science and Engineering Center, Texas Tech University.
- Rhee, D.M., Lombardo, F.T., 2018. Improved near-surface wind speed characterization using damage patterns. *Journal of Wind Engineering and Industrial Aerodynamics* 180, 288–297. <https://doi.org/10.1016/j.jweia.2018.07.017>
- Wurman, J., Kosiba, K., Robinson, P., 2013. In Situ, Doppler Radar, and Video Observations of the Interior Structure of a Tornado and the Wind–Damage Relationship. <https://doi.org/10.1175/BAMS-D-12-00114.1>